**Yoshimura, Hideto; Fujita, Ichiro; Matsushima, Hitoshi**

# Simulation and Image Analysis of Strip Roughness Open-Channel Turbulence with Appreciable Surface Fluctuation

# SIMULATION AND IMAGE ANALYSIS OF STRIP ROUGHNESS OPEN-CHANNEL TURBULENCE WITH APPRECIABLE SURFACE FLUCTUATION


Hideto Yoshimura[1], Ichiro Fujita[2] and Hitoshi Matsushima[3]

[1] Mizuho Information &Research(Graduate School of Science and Technology, Kobe University)
Nishiki-cho,Kanda,Chiyoda-ku,Tokyo,101-8443,Japan e-mail: hideto.yoshimura@mizuho-ir.co.jp
[2] Professor, Department of Civil Engineering, Kobe University
Rokkodai-cho, Nada-ku, Kobe, 657-8501, Japan, e-mail: ifujita@kobe-u.ac.jp
[3]Student, Department of Architecture and Civil Engineering, Kobe University
Rokkodai-cho, Nada-ku, Kobe, 657-8501, Japan, e-mail: 086t140t@stu.kobe-u.ac.jp



## ABSTRACT

Open channel flow with strip roughness is one of the simplest form of rough wall turbulence and the effects of roughness spacing or relative roughness heights have been intensively investigated so far. However, most of the researches concentrate on the flow structure near the roughness elements or frictional relationship between hydraulic parameters and paid little attention to the effects of roughness on water surface. In order to find the relation between surface phenomenon and hydraulic conditions, we performed numerical simulations based on the large eddy simulation (LES) as well as experiments using flow visualization techniques. In the LES, an immersed boundary method is used to represent the effect of strip roughness (Yoshimura, 2007) and the water surface variation is calculated by introducing a density function in a two phase flow simulation. In the experiments, turbulence properties at longitudinal vertical cross-section are measured by PIV technique with the data of surface fluctuation. It was confirmed that the developed LES model is capable to reproduce various types of surface variation observed in the experiments.



*Keywords*: rough-wall turbulence, LES, surface fluctuation, PIV, immersed boundary method


## 1. INTRODUCTION

River surface displays complicated surface pattern depending on various parameters such as water depth, surface velocity, bathymetry as well as the wind speed at the water surface. Additionally, large-scale vortices such as boil vortices or kolk vortices generated at the bottom frequently impinge on the water surface, generating more complicated surface pattern. Despite that these surface patterns are easily observable from bridge or riverbank, numerical simulations for open-channel turbulence have not reproduced those water surface features successfully due to the complexity of near-surface treatment; instead, conventionally water surface has been treated as a rigid-lid boundary not allowing surface fluctuation even in DNS simulations (Lam and Banerjee, 1992, Nagaosa, 1999). Regarding the simulation of rough-wall turbulence, Leonardi et al. (2003), Orlandi et al. (2006) and Ikeda and Durbin (2002) applied DNS to flows with various types of roughness elements; however, these studies treat flow in a duct, not open-channel. As far as the authors' understanding, open-channel flow with rough wall boundary that allows variation or fluctuation of water surface has not been numerically analysed successfully either by LES or DNS. Moreover, the effect of bottom roughness on the water surface fluctuation has not been investigated in detail so far. Therefore, the present research tries to analyse open-channel rough wall turbulent flows by

LES with introducing the density function for the water surface treatment and the immersed boundary method for the treatment of strip roughness element representing roughness used in this study. At the same time, laboratory experiments using the particle image velocimetry (PIV) are performed to visualize and analyse the turbulent properties to compare with the numerical results.

## 2. FLOW VISUALIZATION EXPERIMENT

Figure 1 shows the experimental setup for the PIV experiment. The vertical cross section of the channel is visualized using an Argon ion laser sheet by mixing nylon tracer particles with a diameter of five micron meters. The PIV analysis is performed using three consecutive images captured at a time spacing of 1/500 seconds. In addition, each water surface image is taken from an oblique angle to compare with the simulation afterwards qualitatively. Table 1 shows the hydraulic conditions for the present analysis. $L$ is the distance between each strip roughness, $k$ is the height of the strip roughness set equal to 0.9cm, $Fr$ is the Froude number using the depth from the bottom as a length scale and $Fr_2$ is the Froude number using the depth from the top of the roughness. In the present study, by keeping the mean water depth constant we changed the Froude number by varying the bed slope. As roughness arrangements, the relative spacing, $L/k$, of five and ten are examined.

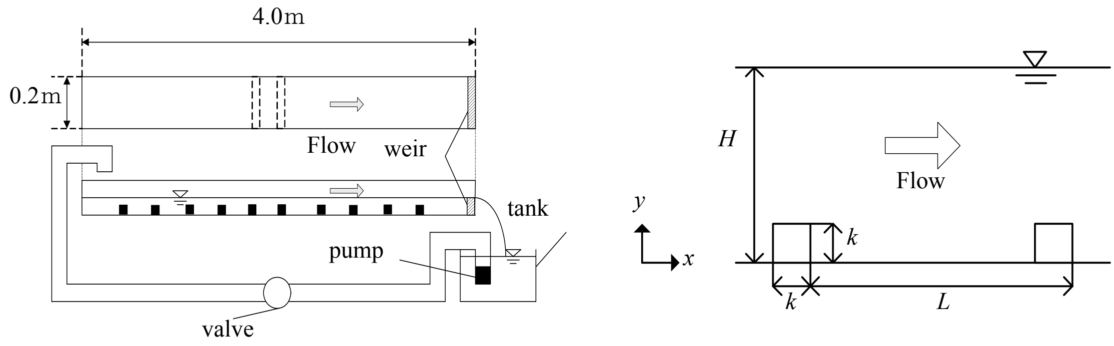


Figure 1 Experimental setup and strip roughness arrangement

Table 1 Hydraulic Conditions

| CASE | Relative spacing $L/k$ | Mean water depth $H$(cm) | Mean velocity $U_m$(cm/s) | Froude number $Fr$ | Froude number $Fr_2$ | Reynolds number $Re$ | Bed slope $I$ |
|---|---|---|---|---|---|---|---|
| L05Fr025 | 5 | 4.0 | 15.625 | 0.25 | 0.366 | 6250 | 1/500 |
| L05Fr04 | | | 25.0 | 0.4 | 0.585 | 10000 | 3/400 |
| L05Fr06 | | | 37.5 | 0.6 | 0.877 | 15000 | 3/200 |
| L05Fr08 | | | 50.0 | 0.8 | 1.170 | 20000 | 11/400 |
| L10Fr025 | 10 | | 15.625 | 0.25 | 0.366 | 6250 | 1/500 |
| L10Fr04 | | | 25.0 | 0.4 | 0.585 | 10000 | 3/400 |
| L10Fr06 | | | 37.5 | 0.6 | 0.877 | 15000 | 3/200 |
| L10Fr08 | | | 50.0 | 0.8 | 1.170 | 20000 | 11/400 |

## 3. NUMERICAL SIMULATION MODEL

In the present study, we modified the previous LES model for strip roughness flow already developed by the first author (Yoshimura, 2007) to represent the relatively large surface fluctuation by using the density function method, one of the gas-liquid two phase models.

### Governing equations

The fundamental equations used in the analysis are the filtered Navie-Stokes equations, the continuity equation and the conservation equation of density function, i.e.,

$$\frac{\partial \overline{u}_i}{\partial t} + \overline{u}_j \frac{\partial \overline{u}_i}{\partial x_j} = -\frac{1}{\overline{\rho}} \frac{\partial \overline{p}}{\partial x_i} + \frac{\partial}{\partial x_i} \left\{ (\overline{\nu} + \nu_t) \left( \frac{\partial \overline{u}_i}{\partial x_j} + \frac{\partial \overline{u}_j}{\partial x_i} \right) \right\} + g_i \tag{1}$$

$$\frac{\partial \overline{u}_i}{\partial x_j} = 0 \tag{2}$$

and

$$\frac{\partial \overline{\phi}}{\partial t} + \frac{\partial (\overline{\phi} \overline{u}_i)}{\partial x_i} = 0 , \tag{3}$$

where $\overline{u}_i$ is the filtered i-component of velocity vector, $\overline{p}$ is the pressure, $g_i$ is the gravitational acceleration in i-direction, $\overline{\rho}$ is the density, $\overline{\nu}$ is the kinematic viscosity, $\nu_t$ is the eddy viscosity, and $\overline{\phi}$ is the density function. The over bar indicates the grid-scale component.

### Immersed boundary method

We introduced the immersed boundary method(IBM) proposed by Fadln et al. (2000) in order to reproduce the shape of the strip roughness in the Cartesian coordinate system. This method expresses the effect of the Dirichlet boundary condition for velocity by introducing the external force in Eq. 1. The discretized form of Eq. 1 by the fractional step method becomes

$$\frac{\overline{u}_i^F - \overline{u}_i^n}{\Delta t} = G_i^n + g_i + \delta_i f_i \tag{4}$$

where

$$G_i = -\overline{u}_j \frac{\partial \overline{u}_i}{\partial x_j} + \frac{\partial}{\partial x_i} \left\{ (\overline{\nu} + \nu_t) \left( \frac{\partial \overline{u}_i}{\partial x_j} + \frac{\partial \overline{u}_j}{\partial x_i} \right) \right\} , \tag{5}$$

$f_i$ is the external force term and $\delta_i$ is a delta function whose value becomes one at point of the velocity boundary condition and zero elsewhere. The external force can be expressed as

$$f_i = -G_i^n - g_i + \frac{U_i^{n+1} - \overline{u}_i^n}{\Delta t} , \tag{6}$$

with

$$U_i^{n+1} = \varphi_i (u_i^{n+1}) . \tag{7}$$

$U_i^{n+1}$ is the boundary velocity at the nearest-to-the-wall grid point calculated from the neighbouring grid point values and the zero velocity at the boundary and $\varphi_i$ is the interpolation operator. By introducing the second order accurate Adams-Bashforth method into Eq. 4 with IBM treatment, we can obtain the following relation

$$[1-\delta_i\varphi_i]u_i^F = [1-\delta_i]\left(u_i^n + \Delta t\frac{3G_i^n - G_i^{n-1}}{2} + g_i\right), \tag{8}$$

from which $u_i^F$ can be calculated. Using the density $\overline{\rho}$ obtained by the density function method the potential function $\overline{p}$ can be calculated from the following Poisson's equation,

$$\frac{\partial}{\partial x_i}\left(\frac{1}{\overline{\rho}}\frac{\partial \overline{p}}{\partial xi}\right) = \frac{\partial u_i^F}{\partial x_i}. \tag{9}$$

The velocity data can be updated using the next relation

$$u_i^{n+1} = u_i^F - \Delta t\frac{1}{\overline{\rho}}\frac{\partial \overline{p}}{\partial x_i}. \tag{10}$$

**The density function method**

The interface between air and water can be captured by introducing the density function to the LES analysis. In the present analysis, the density function $\overline{\phi}$ is basically calculated from the volumetric ratio of water volume $V_l$ to the total volume $V$: i.e., from $\overline{\phi} = V_l / V$. However, since the IBM is introduced in the analysis, the density function is defined both for the fluid phase and for solid phase such that

$$\overline{\phi}_l = \frac{V_l}{V} \tag{11}$$

$$\overline{\phi}_s = \frac{V_s}{V} \tag{12}$$

$$\overline{\phi}_2 = \overline{\phi}_l + \overline{\phi}_s, \tag{13}$$

where the subscripts *l* and *s* denotes the value for fluid and solid, respectively. The density function $\overline{\phi}_2$ becomes zero for the gas phase and one for the liquid phase. The combined density and viscosity are obtained from

$$\overline{\rho} = (1-\overline{\phi}_2)\rho_g + \overline{\phi}_2\rho_l \tag{14}$$

$$\overline{\mu} = (1-\overline{\phi}_2)\overline{\mu}_g + \overline{\phi}_2\overline{\mu}_l \tag{15}$$

where the subscript *g* denotes the value for the gas phase.

**The simulation conditions**

The domain of simulation is 4.5*H* in the streamwise direction *x*, 1.5*H* in the vertical direction *y* and *H* in the horizontal direction *z*, with *H* the mean water depth. The number of grid is (90, 64, 48) in (*x, y, z*) directions. Cyclic boundary conditions are applied in the streamwise and spanwise directions. A slip condition is applied at the top of the gas phase region and a non-slip condition is applied at the bottom boundary. The ratio of gas and liquid densities and that of viscosities are set at $\rho_i/\rho_g = 800$ and $\mu_i/\mu_g = 66.7$, respectively. The third-order-accurate upwind scheme is used in the convection term and a second-order-accurate central scheme is used for the space term discretization. The MTS SGS model (Inagaki et al. 2002) is used for the eddy viscosity model in the calculation of SGS stresses. The simulation is performed in the non-dimensional domain normalized by the mean velocity $U_m$ and the water depth $H$. The non-dimensional time step $\Delta t$ is $5.0 \times 10^{-4}$.

## 4. RESULTS AND DISCUSSIONS

### Water surface variation

Figure 2 presents the instantaneous view of the water surface obtained by the simulation and the experiments for the case of $L/k$=10. The surface variation simulated by the present LES analysis yields quite similar pattern obtained by the experiments except for the small scale capillary ripples superposed on a larger scale variation observable in the photos of experiments. The general agreement of the surface patterns confirms that the introduction of the density function in the LES simulation is successful for the calculation of open-channel flow with strip roughness. In the case of $L/k$=10, the water surface pattern changes significantly as the increase of the Froude number. The water surface is almost flat in the smaller Froude number case of L10Fr025, while for the case of L10Fr04 the surface is deformed into an almost steady two dimensional pattern. Further increase of the Froude number yields three dimensional surface patterns as demonstrated in Figure 2(c) and 2(d). The present LES model is capable to capture such a significant change of surface variation from 2D to 3D pattern fairly well. On the other hand, in the case of $L/k$=5, no appreciable change of surface pattern was observed, which suggests that the bottom roughness arrangement has a great influence on the water surface variation.

.

### Mean and turbulent properties

In the following discussion, we pay attention to the two cases L10Fr04 and L10Fr06 in which water surface displayed relatively large 2D and 3D variations respectively. The mean velocity distributions are compared in Figure 3. The upper row figure shows the time-averaged streamwise velocity distribution and the mean water surface elevation obtained by the simulation. Since the water surface becomes almost steady with standing-wave-like shape in L10Fr04, the equi-velocity lines also shows similar or rather stronger curvature nearer to the water surface. The experimental data by PIV also presents quite similar distribution except the data nearest to the water surface which was difficult to obtain in the present analysis. On the other hand, in the case of L10Fr06, the mean water surface elevation obtained by LES becomes almost flat because the 3D surface ripples change their location from time to time. Therefore the velocity distribution becomes quite different from that in L10Fr04. On the contrary, velocity distributions near the bottom show almost the same pattern between the cases, suggesting that the mean flow structure near the bed does not receive a strong influence from the flow near the surface.

The Reynolds stress distributions are shown in Figure 4. In each case, the Reynolds stress takes the maximum value along the shear layer developed downstream of the strip roughness and does not seem to have an appreciable impact from the water surface fluctuations.

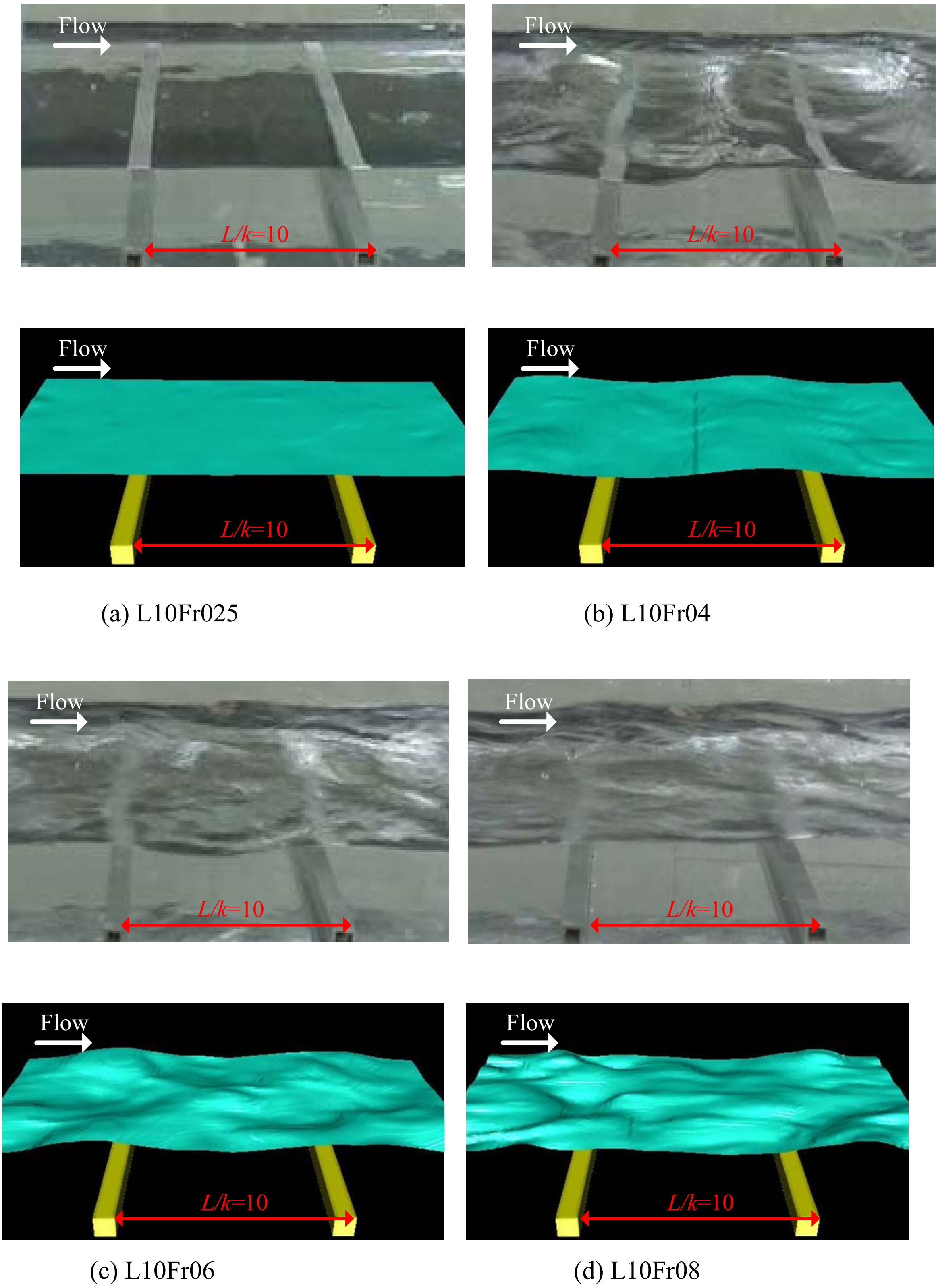


Figure 2 Comparison of surface variation (upper: experiment, lower: LES)

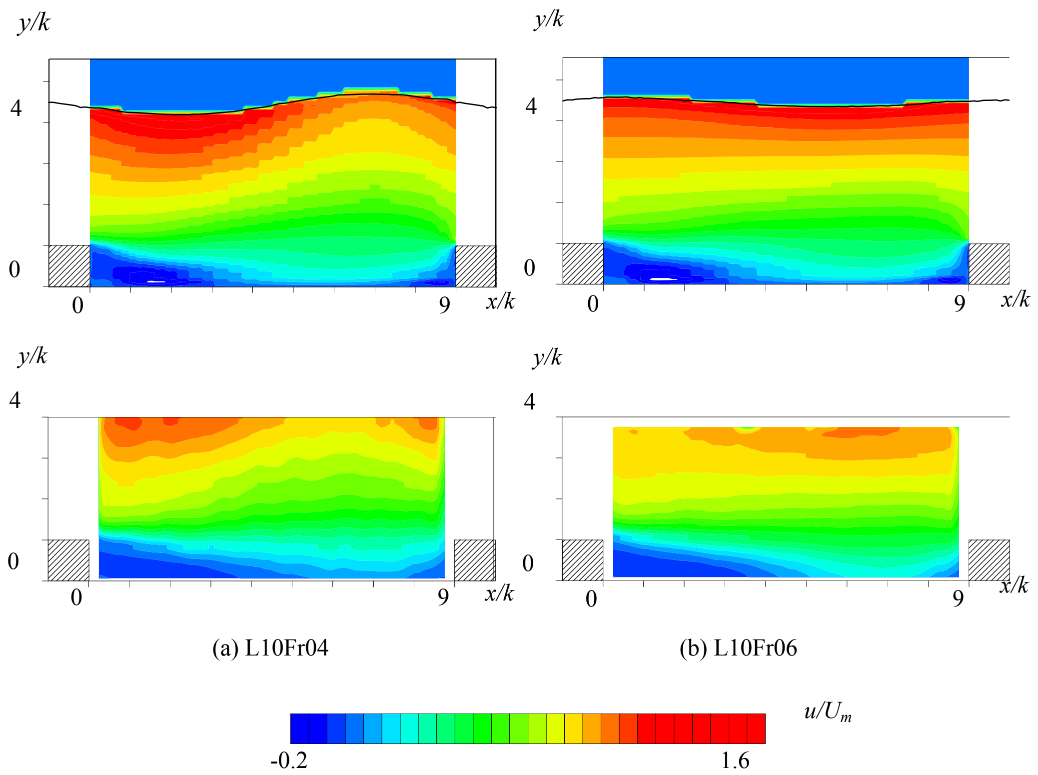


Figure 3 Mean velocity distribution (upper: LES, lower: PIV)

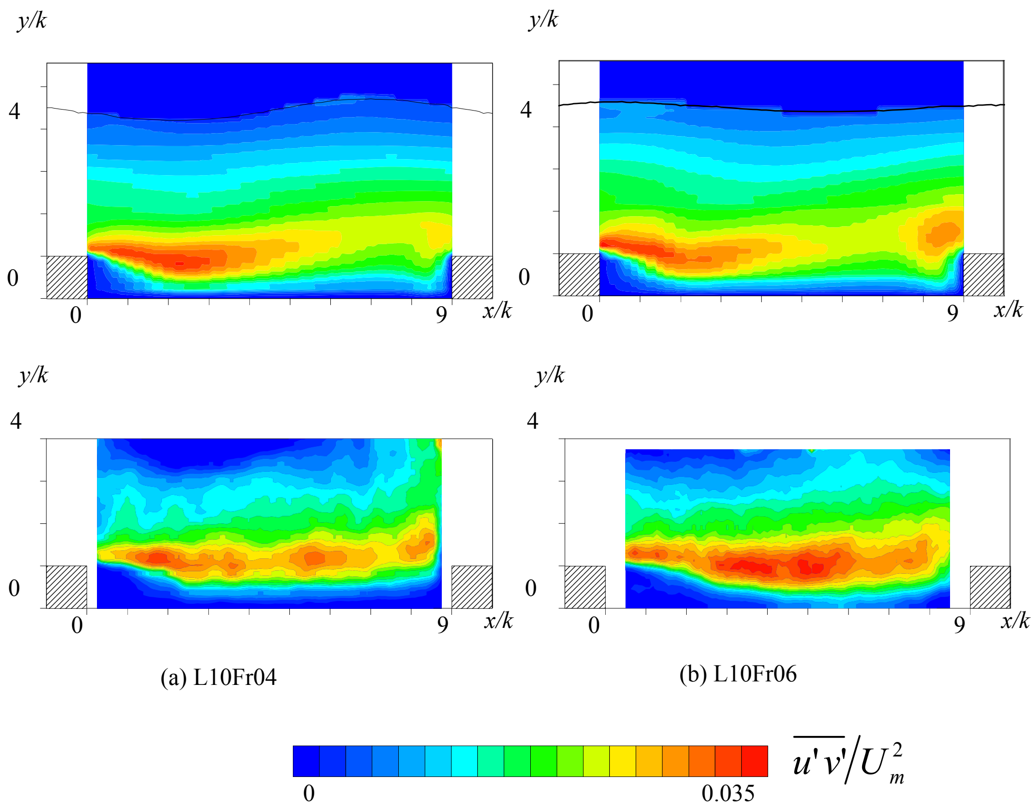


Figure 4 Reynolds stress distribution (upper: LES, lower: PIV)

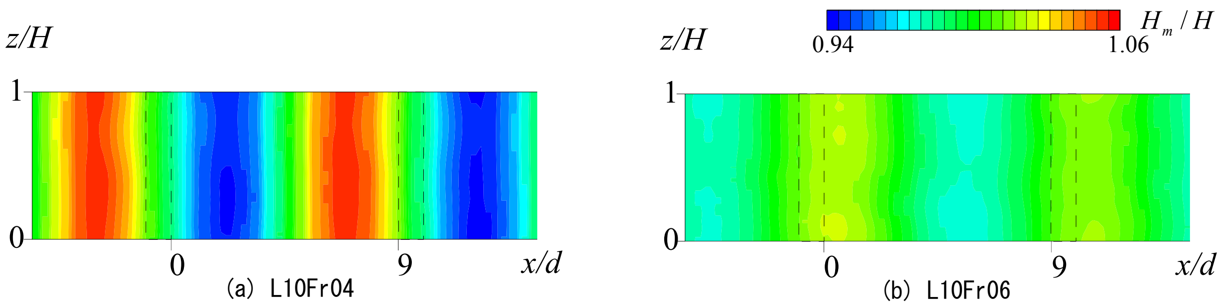


Figure 5 Mean depth variation by LES

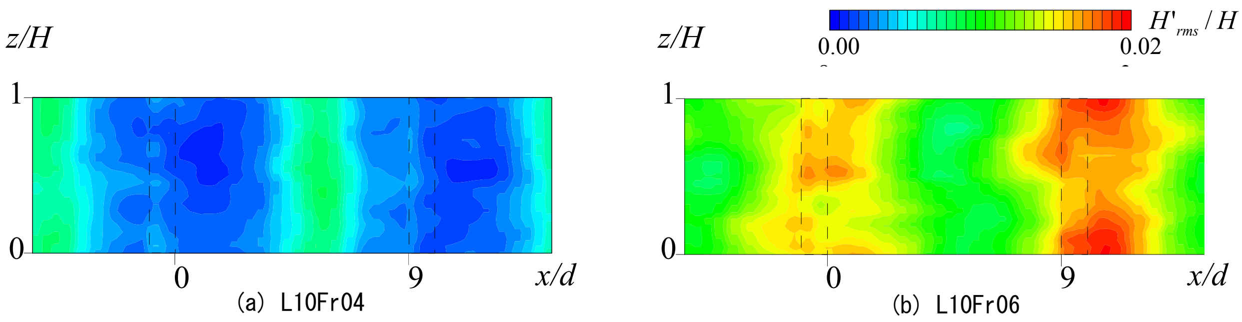


Figure 6 Surface fluctuation intensity by LES

**Water surface fluctuation**

The average water depth distributions calculated by LES are shown in Figure 5. As already discussed previously, the case L10Fr04 includes a relatively large surface variation having a peak water level just upstream of the strip roughness, while in L10Fr06 the water surface variations are cancelled out yielding planar distribution after averaging with a slight increase of water level just downstream of the strip roughness. The intensity distributions of water surface fluctuation are indicated in Figure 6. In contrast to the averaged data, the L10Fr06 shows a larger variation than L10Fr04 because the time-dependent surface variation is much larger than that in L10Fr04 in which the surface level is kept constant steadily. It should be noted that in L10Fr06 the maximum intensity appears just downstream of the strip roughness location where the average water level displayed a slight increase. This suggests that the upwelling vortices generated near the bottom are more intensively hitting the water surface in this zone, which has to be investigated in a further research. Figure 7 presents the surface fluctuation intensities averaged between the strip roughnesses. Here the experimental data of Nezu and Nakayama (2004) for a smooth bed are compared. Also shown are the data with respect to the case of Fr=0.7 which was not treated in the previous discussions. Allowing the scatter of the data in between the case, the general feature of the surface fluctuation intensity showing increase with the Froude number is verified fairly well.

## 5. CONCLUSIONS

The present study made analyses of open-channel flow with strip roughness in terms of the large eddy simulation and the particle image analysis. The developed LES model is capable of estimating water surface fluctuations using the density functions; i.e., the water surface is treated as the interface between the gas and the liquid phases. The simulated results agreed fairly well with the experiments with respect to the mean and turbulent properties of velocity field and water-surface field. It was made clear from the experiment and simulation that for the case of a relatively large strip roughness spacing, $L/k$=10, the water surface pattern changes from 2D to 3D configurations as the increase of the Froude number; while for the smaller roughness spacing water surface pattern shows no significant difference with the Froude number. On the other hand, turbulent properties near the bed present almost the similar pattern even when the water surface configuration becomes 2D or 3D; e.g. the length of the reattachment point is almost the same irrespective of the water surface shape. However, for the case in which the intensity of surface fluctuation displays local maxima, L10Fr06, the mean water surface also indicates a slight increase at the same local location, suggesting the existence of the interaction of water surface and bottom vortex separated at the strip roughness. Further research is required for understanding the correlation between surface fluctuation and vortices generated near the bed.

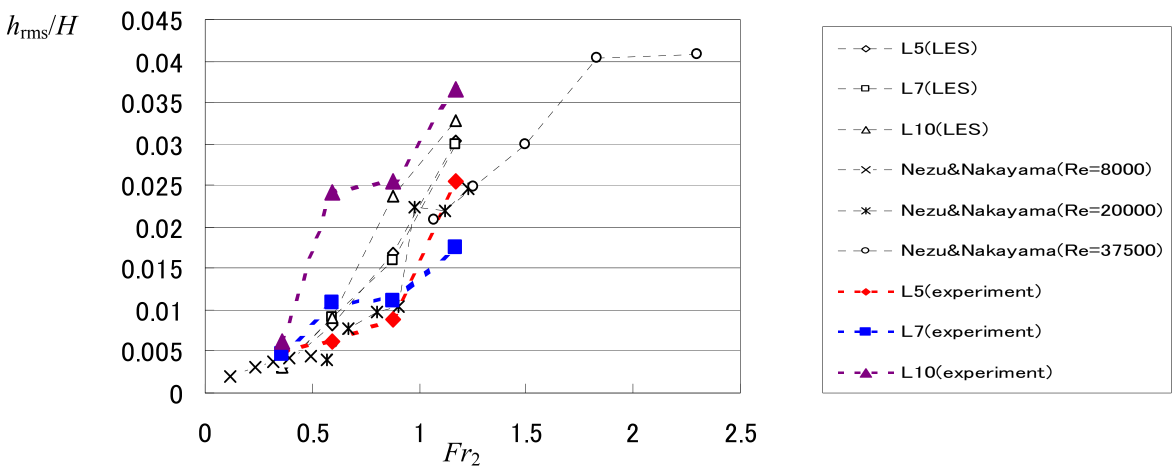


Figure 7 Water surface fluctuations

## REFERENCES


Fadln,E., A., Verzicco, R., Orlandi, P. and Mohd-Yusof, J. (2000), Combined Immersed-Boundary Finite-Difference Methods for Three-Dimensional Complex Flow Simulations, *J. Comp. Phys.* ,161-1, pp.35-60.

Ikeda, T. and Durbin, P.A. (2002), Direct simulations of a rough-wall channel flow, Report No.TF-81, *Flow Physics and Combustion Division,* Stanford University.

Inagaki, M., Kondoh, T. and Nagano, Y. (2002), A mixed-time-scale SGS model with fixed model-parameters for practical LES, *In Engineering Turbulence Modelling and Experiments 5* (Edited by Rodi, W. and Fueyo, N.),Elsevier, pp.257-266.

Lam, K. and Banerjee, S. (1992), On the condition of streak formation in a bounded turbulent flow, *Phys. Fluids* , A4-2, pp.306-320.

Leonardi, S., Orlandi, P., Smalley, R., J., Djenidi, L. and Antonia, R.,A. (2003), Direct numerical simulation of turbulent channel flow with transverse square bars on the wall, *J. Fluid Mech.* ,Vol.491, pp.229-238.

Nagaosa, R. (1999), Direct numerical simulation of vortex structures and turbulent scalar transfer across a free surface in a fully developed turbulence, *Phys. Fluids* , 11-6, pp.1581-1595.

Nezu, I. and Nakagawa, T.(1998), Relationship between turbulent structure near the free-surface and surface-wave fluctuations, *Journal of Hydraulic, Coastal and Environmental Engineering JSCE*, Vol.593, II-43, pp.69-78.(in Japanese)

Orlandi, P., Leonardi, S. and Antonia, R.,A. (2006), Turbulent channel flow with either transverse or longitudinal roughness elements on one wall, *J. Fluid Mech.* ,Vol.561, pp.279-305.

Yoshimura, H. (2007), Analysis of open-channel flow with strip roughness by LES using immersed boundary method, *Proceedings of the 32nd IIHR congress*, on CD-ROM.